Smart Textile Reinforced Concrete Sensory Structures

Yiska Goldfeld, Oded Rabinovitch, Till Quadflieg, Barak Fishbain, Thomas Gries

SMART TEXTILE REINFORCED CONCRETE SENSORY STRUCTURES

Yiska Goldfeld[1], Oded Rabinovitch[1], Till Quadflieg[2], Barak Fishbain[1], Thomas Gries[2]

[1] Faculty of Civil and Environmental Engineering, Technion –Israel Institute of Technology
Haifa, 32000, Israel.
[2] Institut fuer Textiltechnik, RWTH Aachen University, Aachen, 52074, Germany

yiska@tx.technion.ac.il

ABSTRACT

This study examines and demonstrates the feasibility of a new class of smart textile reinforced concrete (TRC) structural elements with inherent sensing capabilities that are based on embedding metallic yarns in the textile mesh. The new approach combines the advantages of thin walled glass fiber based TRC with the electro-mechanical properties of the stainless steel fibers embedded in the textile matrix. To examine this concept and to demonstrate its potential feasibility, TRC beam specimens are tested and monitored under mechanical and environmental loading condition. The results of the tests demonstrate the features of the sensory/structural system, reveals its potential use as a basis for a combined structural and functional monitoring system, and highlights its spectrum of potential applications.

KEYWORDS : *Textile reinforced concrete (TRC); structural health monitoring; sensing; intelligent structures; structural mechanics.*

INTRODUCTION

The development of intelligent concrete structures is a great challenge and opportunity of today's structural engineering. Social requirements such as significant and meaningful reduction of consumption of natural materials demand the development of effective and safe lightweight concrete structures. The need to mitigate the impact of catastrophic events such as earthquakes, tsunamis, storms, or acts of terror and, at the same time, to provide the society with sustainable structures also calls for better material utilization on one hand and for advanced sensing and monitoring techniques on the other. Today, concrete structures with sensing abilities consist of three components: the structural system, the health monitoring system, and the functionality monitoring system. Tomorrow's intelligent structure will be a single multifunctional physical element that addresses all tasks at once.

Fiber reinforcement for Textile Reinforced Concrete (TRC) ranges from glass and carbon to steel fibers. The combination of metallic and glass fibers reduces the amount of reinforcement considerably and make cost-effective structures achievable [1-2]. Monitoring techniques for RC elements range from traditional ones such as visual inspection or tap tests, to modern techniques based on embedded or surface mounted strain sensors. Strain sensors are either localized such as fiber Bragg grating, or distributed such as fiber optics [3-6]. For the use in sensory TRC elements fiber Bragg grating sensors can be installed on a woven textile [7]. For geotechnical applications, technical textiles can deploy optical time-domain reflectometer (OTDR) sensors [8]. Warp knitted textile as reinforcing textile for sensory TRC elements can include threads of metallic wires to provide the system with the sensory capacity, see, for example, [9].

All common methods used for monitoring are based on implementation of an additional sensing system in a structural element. The additional sensing system occupy space with the load-bearing element and provides the potential of degradation of effective properties of the host element. The clear distinction between the structural system and the sensory one makes further interpretation of the signal necessary. The sensor itself is commonly expansive and its implementation is costly, time-consuming, and it requires specially trained personnel.

The current study faces this challenge and explores the feasibility of a sensory textile reinforced concrete (TRC) structural element with inherent sensing capabilities. Opposed to the organic materials used in [2], the new concept uses glass and stainless steel fiber textiles as reinforcement for a TRC element and utilizes the electric/strain behavior of the stainless steel fibers as a basis for its sensory feature. The structural and sensing system is examined in two scenarios. The first one involves mechanical loading of a sensory TRC beam specimens and focuses on the structural monitoring capabilities of the system. The second scenario examines the response of the sensory TRC system to wetting and to penetration of water through cracks. This aims to explore the multifunctional nature of the system and its ability to monitor the interaction with a water.

1 TEXTILES WITH EMBEDDED STAINLESS STEEL SENSORY YARNS

The sensory textile combines tows made of glass fibers and yarns made of stainless steel ([1], [8]). The glass tows, which are organized in a warp knitted grid structure with a mesh size of 7-8 mm, are the main reinforcement platform. The stainless steel fibers are embedded in that main reinforcement layer. At the same time, the stainless steel yarns are used as the sensory agent. The density of the glass fiber tows is 2,400 tex and it is made of alkali resistant (AR) glass fibers. The properties of the tows are: specific mass=2,680 kg/m^3, modulus of elasticity=72 GPa, tensile strength=1,700 MPa. The equivalent diameter equals 1.06mm. The metallic yarns are made of stainless steel 12μm filaments in two twisted yarns (275X2), 75 N maximum load, 14 Ohm/m resistance, and maximum strain of 10%.

Figure1: Conductive thread insertion into warp knit.

The production of the multi-material textile is illustrated in Figure 1. The production process was not involved with any modifications in terms of tribology or tension control of the fibers. This demonstrates that the embedment of the sensory agents by their implementation as an additional component of the textile does not introduce significant complexity to the textile manufacturing procedure. The layout of the textile was designed to assure its suitability for application as reinforcement for TRC elements. These two aspects demonstrate that the conversion of the textile into a sensory one does not necessitates significant changes to the conventional procedures, either for the textile itself or for the textile reinforced concrete (TRC) member element. Correspondingly, the cost associated with the conversion into a sensory system is not expected to be a significant factor.

2 SENSORY TRC STRUCTURAL ELEMENTS

This section examines the feasibility of the textile reinforcement with the embedded metallic sensory agents. Opposed to preliminary tests and experiments, which focused on the component level and mainly on the strain sensing capabilities of the metallic yarns [9], here we look at the structural element level. The shift form the component level to the higher structural element is achieved by designing, casting, testing, and analyzing TRC beams (also see [2]). These essential steps in the examination and potential demonstration of the concept are outlined next.

2.1 Design and production of TRC beam samples

Two beam samples reinforced with the sensory textile (i.e. the glass tows textile with the embedded stainless steel sensory yarns) have been designed and casted (also see [2]). The two beams are referred to as Beam M1 and Beam M2 and their general layout is shown in Figure 2. The beams are 280 mm

long, 70 wide, and 30-35 mm thick and they are reinforced with three layers of textile. The details of the textile layers and their locations are also shown in Figure 2. Each textile layer includes 6 longitudinal (0°) tows of glass fibers. Beam M1 includes one stainless steel yarn per layer and Beams M2 includes two stainless steel yarns per layer. The transverse (90°) tows are all made of glass fibers. In attempt to keep the textile layers in place during casting, to allow smooth flow of the concrete (grout) mix, and to avoid segregation, the textile layer were slightly pre-tensioned.

In order to use a standardized product that can be easily reproduced in other laboratories, and in order to work utilize the high strength, short curing times, good workability, and improved rheological properties, a commercial grout mixture (Sika Grout 214) was adopted for casting the beams. The mixture was prepared in accordance with the manufacturer instructions. The beams were cured in room temperature and normal moisture conditions. The tensile strength and the compressive strength of the grout were determined as 59.4 MPa through standard bending and compression tests on 160x40x40 mm prisms. These results are in agreement with the data provided by the manufacturer.

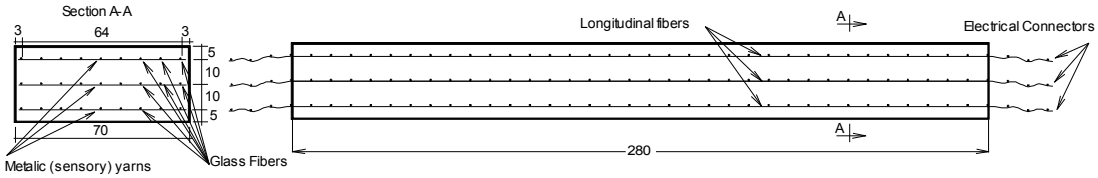

Figure 2: Drawing of the beam.

2.2 Mechanical and electrical test setup

The mechanical testing of the beams was conducted in a displacement control mode with a loading rate of 0.25 mm/min. The beams were tested to failure in a four point bending scheme as illustrated in Figure 3. Along with the monitoring of the internal sensory textile, the test included monitoring of the load; the crosshead location; the vertical displacement at the middle of the beam, and the strains at the upper and lower faces of the beams. The latter were measured by two 60 mm long strain gauges. The monitoring capabilities of the stainless steel yarns are based on detecting changes to their electrical resistance. The change in resistance is inferred from the voltage difference across a Wheatstone bridge. Thus, in the scope of this study, the monitoring of the voltage difference across the bridge is discussed. The layout of the Wheatstone bridge and the properties of its components link a resistance change of up to 18[mΩ] to voltage change of up to 100[μV].

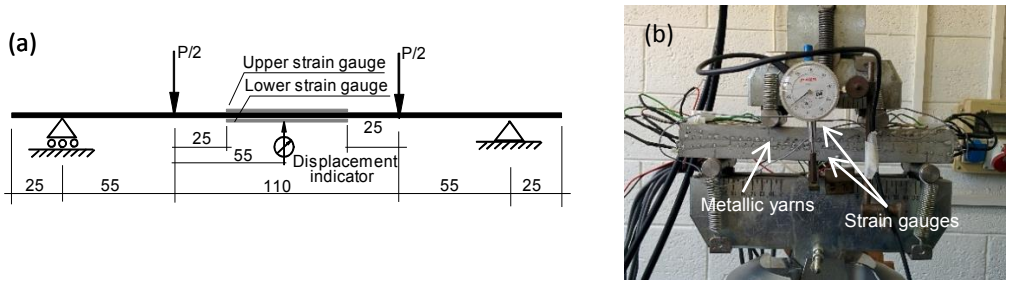

Figure 3: (a) Loading scheme and "external" sensing (adapted from [2]); (b) Test specimen and testing rig.

2.3 Characterization of the structural response of the TRC beams

The characterization of the response of the beam to the mechanical load focuses on the load-displacement curve and on the strains measured by the various sensory devices. This effort aims to characterize the structural behavior of the TRC beam. Then, the ability of the embedded metallic sensors to capture and quantify the process is examined. Figure 4 depicts the load versus deflection curve and the readings of the two external strain gauges for the two beams. Although the reference strain measurements are limited to the outer faces of the beam, the classical assumption of a linear strain distribution allows assessing the variation of the strains through the thickness of the beam:

$$\varepsilon(z) = \frac{\varepsilon_b + \varepsilon_t}{2} + \frac{\varepsilon_b - \varepsilon_t}{H} z \quad (1)$$

where $\varepsilon(z)$ is the distribution of strains; ε_t and ε_b are the strains at the upper and lower faces of the tested beam measured by the strain gauges; H is the height (thickness) of the beam; and z is the vertical coordinate. Pictures of the tested beams at intermediate stages of loading appear in Figure 5.

The load-deflection curves and the strain response curves (Figure 4) reveal three main phases in the structural response of the TRC beams. The first one includes the initial response of the un-cracked beam. After the initial settlement of the test setup, this phase reveals a linear response. This phase extends up to a load level of about 2.5 kN (point A) for beam M2 and 1.9 kN for beam M1, where the first flexural cracks are detected. The cracking from this point and on is well reflected by the changes of the slopes of the load-deflection and strain evolution curves.

The second phase starts after the first cracking at Point A. The formation of flexural hairline cracks yields a reduction in the stiffness of the beam manifested by the slope of the load deflection curve and the increased rate of strain evolution. The flexural cracking and the resistance of the global bending moment through compression in the concrete and tension in the reinforcing textile also shifts the height of the natural axis upwards. Consequently, the tensile strains at the lower face grow much faster than the compressive ones at the upper face, see Figure 4.

The cracking pattern detected in the second phase includes a series of distributed hairline flexural cracks. The number of cracks increases with a further increase in load deflections. This effect reflects a sound mechanical anchorage and an effective bond between the textile and the concrete. It also reflects a favorable behavior in terms of durability and structural response at the post-cracking stage.

The third phase of the structural response starts at a load level of about 2.9 kN for beam M2 and 2.37 kN for beam M1 (point B in Figure 4). Here, the load slightly drops down with the opening of one major shear-flexure crack that develops under the right loading point (see Figure 5). The phase involves a gradual reduction in the slope of the load-deflection curve up to the peak load (Point C) and then a monotonic reduction in load up to the point where the test has been terminated. The tensile strains at the lower face of the beam (Figure 4) reveal a similar pattern. These observations are typical to beams of such aspect ratios at the ultimate state.

During the entire test, the reinforcing textile kept bridging the opening cracks. Rupture or pull out of the reinforcement were not observed. This clarifies that the textile reinforcement provides the structural element with the ability to maintain its functionality close to failure without a sudden release of load. This effect further demonstrates the structural capabilities of the TRC element and draw the attention to its sensory capabilities.

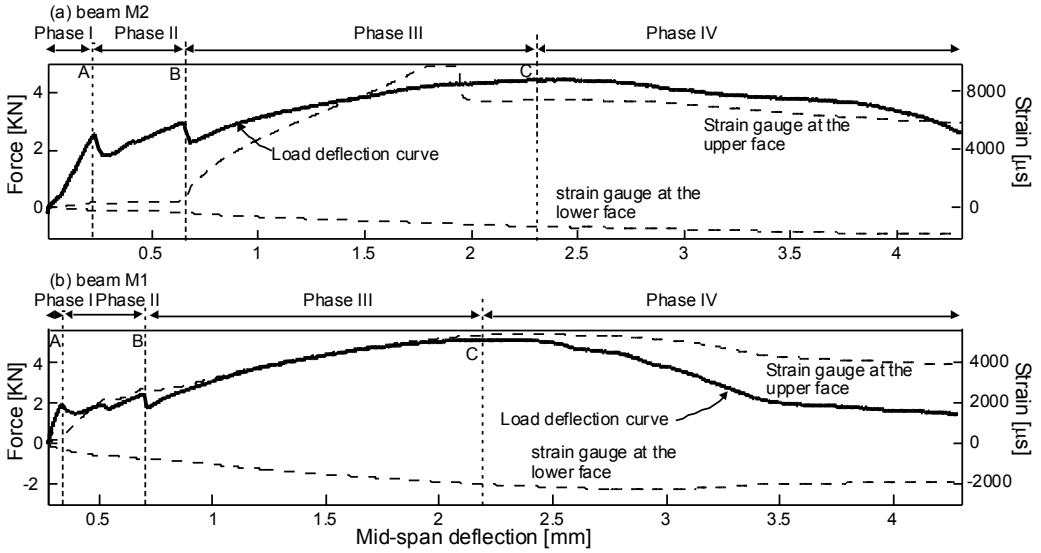

Figure 4: Load-deflection curves and readings of the strain gauges: (a) beam M2, (b) beam M1.

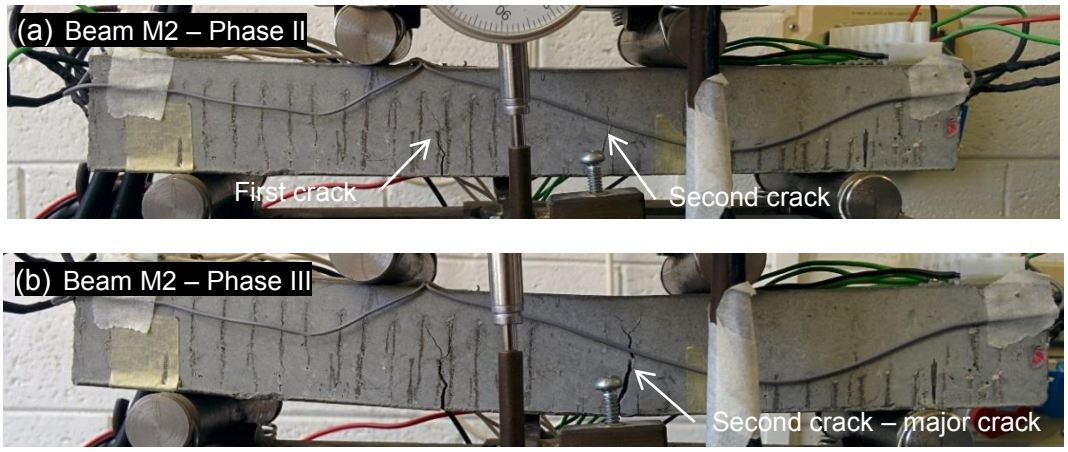

Figure 5: Beam M2 at different stages of the loading process: (a) Phase II; (b) Phase III.

2.4 Sensing Capabilities: Readings of the metallic sensors

The analysis of the sensing capabilities looks into the electrical reading of the metallic yarns. The normalized electrical readings are plotted and qualitatively compared with the normalized load-deflection curve in Figures 6 and 7 (for beams M2 and M1, respectively). All curves are normalized to the non-dimensional range of 0 to 1. This representation aims to examine the correlation between the electrical readings of the sensor and the mechanical behavior of the beam, as reflected by the load-deflection curve. Figures 6a and 7a refer to the metallic yarns near the upper face of each beam. Figures 6b and 7b refer to the yarns near the middle of each beam and Figures 6c and 7c refer to the yarns near the lower faces. The discussion is limited to the ascending loading branch up to point B.

The normalized readings reveal that the sensory yarns provide relevant information regarding the structural behavior of the tested beam. The most important aspect of the response is the behavior of the tensed textile located near the lower face of the beam. Indeed, Figures 6c and 7c show that the electrical readings of the lower metallic yarns well detect the initiation of cracking at point A. This event is reflected by the changes to the slope of the normalized electrical curve. Due to their location near the compressed and the neutral regions of the beam, the correlation of the compressed (Figures 6a and 7a) and middle (Figures 6b and 7b) yarns is not as good as the one of the tensed yarn. This effect is attributed to the small absolute value of strains detected near the middle of the beam and the exposure of the upper yarns compression. Yet, the tensed yarns clearly and effectively detect the main features of the structural response of the beam. Figure 6 also reveals that in the beam tested with two adjacent metallic yarns (Beam M2), the normalized electrical readings of one yarn are very close to the reading of the other. This is another indication of the relevance of the readings, the consistency of the monitoring technique, and the potential ability to use the TRC element as a sensory structural component. The quantitative aspects of this potential are discussed next.

2.5 Sensing Capabilities: Calibration of the sensory textile

In order to examine the quantitative capabilities of the sensory system, the electrical readings detected by the metallic yarns are calibrated using the interpolated strains (Equation 1) in phase I. The calibrated results appear in Figure 8 for beam M2 and in Figure 9 for beam M1. In both cases, the levels of strain detected near the middle of the beam are very low and therefore they are not shown. In both cases, the calibrated results reveal a good level of correlation, particularly in terms of the ability to quantitatively detect the strains near the tensed face of the beam. It is also revealed that in each beam, the same calibration factors (which are listed in the figure) hold for the tensed and the compressed fibers. On the other hand, the calibration factors differ from one beam to another. This effect is mainly attributed to the different levels of strains detected by the external strain gauges mounted on the two beams (Figure 4). Comparing Figure 4a with Figure 4b reveals that the strain

values detected in beam M2 are about two times larger than the ones in beam M1. Correspondingly, the calibration factor for beam M2 (45 ε/μV) is about twice as large as the factor for beam M1 (25 ε/μV). In that sense, the discrepancy is not necessarily attributed to the sensory system but to other factors affecting the readings of the external strain gauges. Bearing that in mind, it appears that the sensory TRC system that is based on the metallic yarns can indeed monitor quantitative and relevant information about the structural state of the element.

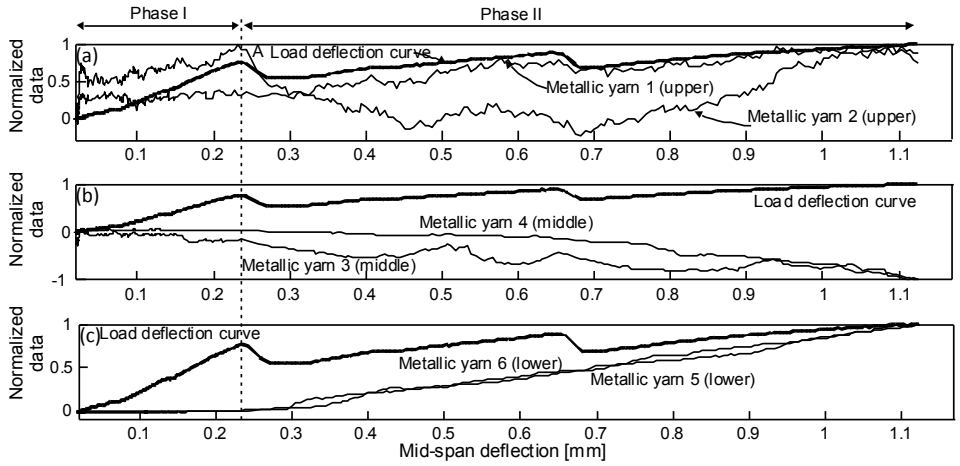

Figure 6: Normalized electrical readings of the metallic yarns in beam M2 and normalized applied load versus mid-span deflection: (a) upper metallic yarns; (b) middle metallic yarns; (c) lower metallic yarns.

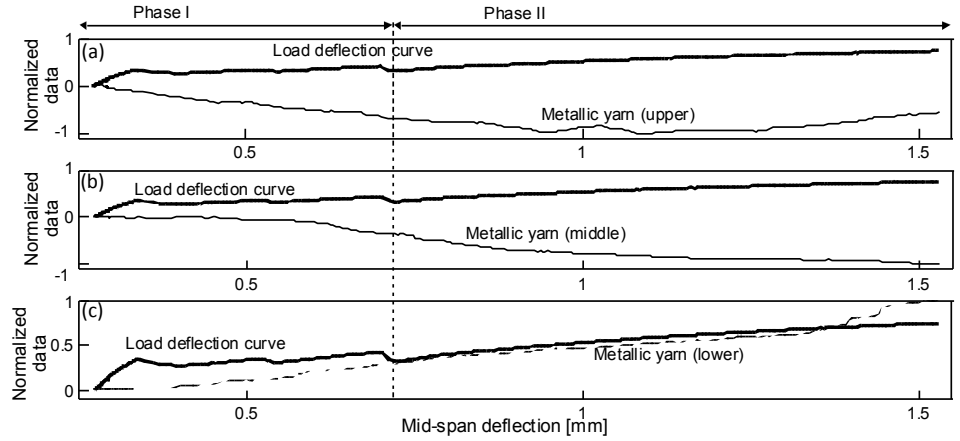

Figure 7: Normalized electrical readings of the metallic yarns in beam M1 and normalized applied load versus mid-span deflection: (a) upper metallic yarns; (b) middle metallic yarns; (c) lower metallic yarns.

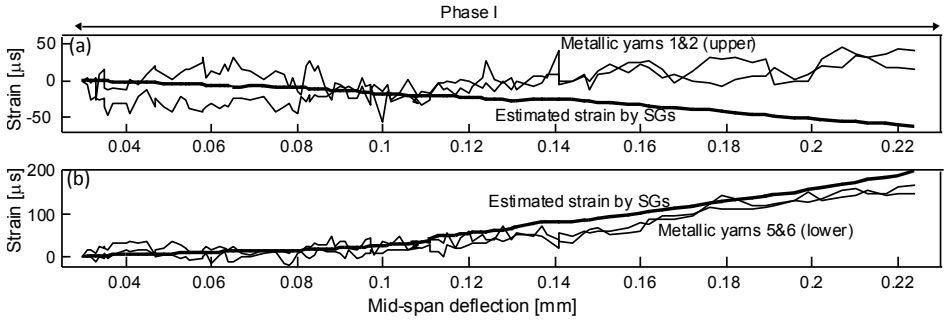

Figure 8: Strain reading of the metallic yarns in beam M2 compared with strains interpolated using the readings of the strain gauges (calibration factor=45 ε/μV): (a) upper yarns; (b) lower yarns.

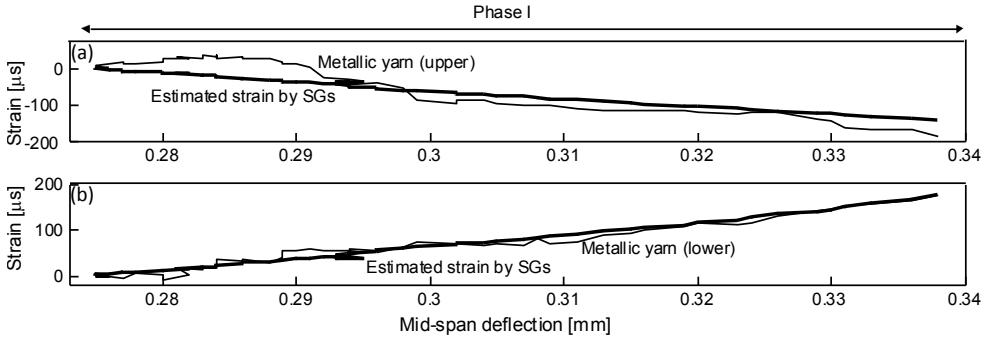

Figure 9: Strain reading of the metallic yarns in beam M1 compared with strains interpolated using the readings of the strain gauges (calibration factor=25 ε/μV): (a) upper yarns; (b) lower yarns.

2.6 Sensing Capabilities: Response to wetting with tap water

The last aspect of the sensory system focuses on its response to environmental conditions. Specifically, it looks into its exposure to wetting with tap water and its ability to electrically detect such event. This ability is important in terms of monitoring the functionality of structural systems that are exposed to an aquatic environment (water and wastewater pipelines, marine structures, wastewater treatment facilities, etc.) as well as in terms of detecting cracks in the TRC element, also see [2].

The normalized electrical response of beam M2 to three wetting events is studied in Figure 10. In the first event (t=60 sec), the un-cracked part of the beam is wetted. The normalized electric readings are insensitive to this even and they do not reveal any significant change to the signal. On the other hand, in the second event (t=160 sec), the region where small cracks (first crack in Figure 5a) have developed was wetted. In this case, the sensory system reveals a significant reading in terms of jumps in the normalized voltage curves. This observation becomes even more significant in the third event where the major crack has been exposed to tap water (t=260 sec). This scenario yield significant jumps in all electrical readings, including those of the compressed yarns. These observations clearly indicate that the sensory yarns, originally implemented in the TRC system in attempt to monitor the structural health in terms of strains and cracking, can also detect wetting and penetration of water through cracks. As such, it can monitor the functionality of the system and may turn to be an effective mean to detect leakage in water supply systems.

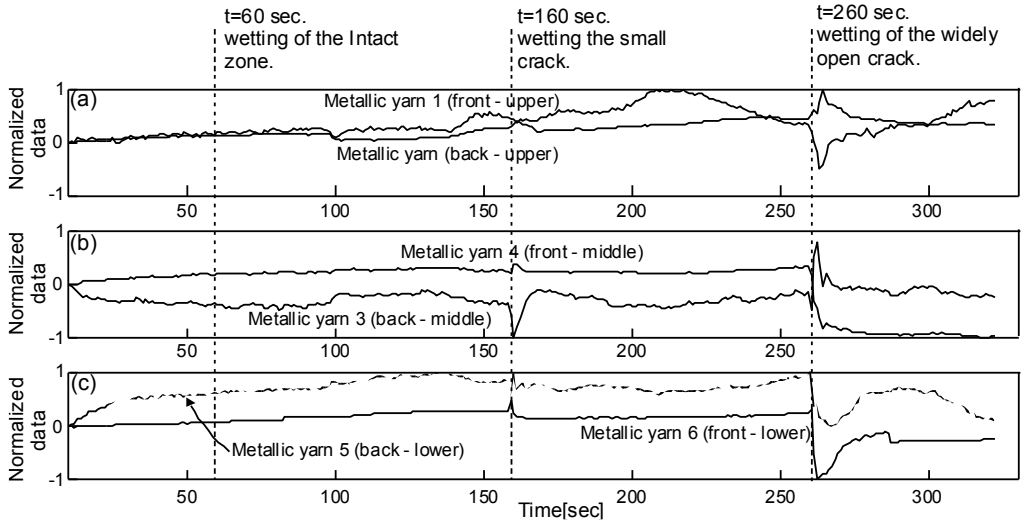

Figure 10: Wetting test of beam M2: (a) lower face; (b) middle; (c) upper face.

CONCLUSIONS

In this paper, the potential use of glass fiber based textile reinforcement with embedded stainless steel yarns for the structural health monitoring and functional monitoring of TRC elements has been investigated. The paper has experimentally demonstrated that the integrated textile can be effectively used for the detection of the major structural events in the response of TRC beams and for the assessment of the levels of strains that evolve within the beam. The latter has been achieved by introducing the metallic yarns into a bridge configuration, by monitoring the changes to the voltage across the bridge, and by simple scaling, normalization, and calibration of the raw monitored data.

Along with the potential structural health monitoring capabilities of the metallic/glass textile reinforced concrete element, the paper has also revealed its potential functional monitoring feature. Specifically, it has been shown that once the concrete element is cracked, the sensory system can effectively detect its exposure to water. This ability paves the way to a broad spectrum of applications ranging from leakage detection to crack detection in structural systems that are normally exposed to aquatic environments.

The simplicity of the monitoring procedures outlined here, the ability to implement the metallic components through standard and conventional textile manufacturing procedures, the minimal modifications to the manufacturing and casting procedures, and the minimal cost associated with the conversion of a standard TRC element into a sensory one are potential advantages of the approach propose here. On the other hand, this approach raises many other questions and highlights many aspects that still have to be clarified. Together, these challenges define new and additional research directions in this field.

ACKNOWLEDGMENT

The financial support from the Umbrella Cooperation Program of the Technion and RWTH Aachen University is gratefully acknowledged. The authors are also grateful for the help of Barak Ofir, Elhanan Yitzhak, and the stuff of the National Building Research Institute at the Technion.

REFERENCES

[1] Hegger, J., Golralski, C. Kulas M, C., Schlanke Fußgängerbrücke aus Textilbeton –Sechsfeldrige Fußgängerbrücke mit einer Gesamtlänge von 97 m, *Beton und Stahlbau*, 106(2), 64-71, 2011.

[2] Goldfeld, Y., Rabinovitch, O., Quadflieg, T., Fishbain B., Gries, T., New Concept of Carbon Fiber Based Sensory Textile Reinforced Concrete for Smart Structures, submitted 2014.

[3] Majumder, M., Gangopadhyay, T. K., Chakraborty, A. K., Dasgupta, K. Bhattacharya D.K., Fibre Bragg gratings in structural health monitoring—Present status and applications, *Sensors and Actuators A: Physical*, 147(1), 150-163, 2008.

[4] Li, H-N., Li, D-S., Song, G-B. Recent applications of fiber optic sensors to health monitoring in civil engineering, *Engineering Structures*, 26(11), 1647-1657, 2004.

[5] Lee, B., Review of present status of optical fiber sensors, *Optical Fiber Technology*, 9, 57-79, 2003.

[6] Khotiaintsev, S., Beltrán-Hernández, A., González-Tinoco, J., Guzmán-Olguín, H., Aguilar-Ramos, G., Structural health monitoring of concrete elements with embedded arrays of optical fibers, *SPIE Conference on Health Monitoring of Structural and Biological Systems 2013*; San Diego, CA; United States; 11-14 March 2013; Volume 8695, Article number 869513.

[7] Montanini, R. , De Domenico, F., Freni, F., Maugeri, N., Recupero, A., Structural health monitoring of reinforced concrete beams by means of embedded fiber Bragg grating sensors, *22nd International Conference on Optical Fiber Sensors*; Beijing; China; 15-19 October 2012, V. 8421, Article no. 8421AW.

[8] Krebber, K., Lenke, P., Liehr, S., Nother, N., Wendt, M., Wosniok, A., Daum, W., Structural Health Monitoring by Distributed Fiber Optic Sensors Embedded into Technical Textiles, *Bauwerksuberwachung mittels technischer Textilgewebe mit integrierten faseroptischen Sensoren*, 2012.

[9] Quadflieg, T., Tomoscheit, S., Gries, T., Humidity and Strain Monitoring for Textile Reinforced Concrete, *Second Conference on Smart Monitoring, Assessment and Rehabilitation of Civil Structures*, Istanbul, Turkey, 9-11 September 2013.